Accepted Manuscript

Title: Suppression of the release of arsenic from arsenopyrite by carrier-microencapsulation using Ti-catechol complex

Authors: Ilhwan Park, Carlito Baltazar Tabelin, Kagehiro Magaribuchi, Kensuke Seno, Mayumi Ito, Naoki Hiroyoshi

PII: S0304-3894(17)30781-1
DOI: https://doi.org/10.1016/j.jhazmat.2017.10.025
Reference: HAZMAT 18930

To appear in: *Journal of Hazardous Materials*

Received date: 8-4-2017
Revised date: 24-9-2017
Accepted date: 12-10-2017

Please cite this article as: Ilhwan Park, Carlito Baltazar Tabelin, Kagehiro Magaribuchi, Kensuke Seno, Mayumi Ito, Naoki Hiroyoshi, Suppression of the release of arsenic from arsenopyrite by carrier-microencapsulation using Ti-catechol complex, Journal of Hazardous Materials https://doi.org/10.1016/j.jhazmat.2017.10.025

This is a PDF file of an unedited manuscript that has been accepted for publication. As a service to our customers we are providing this early version of the manuscript. The manuscript will undergo copyediting, typesetting, and review of the resulting proof before it is published in its final form. Please note that during the production process errors may be discovered which could affect the content, and all legal disclaimers that apply to the journal pertain.

ACCEPTED MANUSCRIPT

Suppression of the release of arsenic from arsenopyrite by carrier-microencapsulation using Ti-catechol complex

Ilhwan Park[a, †, *], Carlito Baltazar Tabelin[b, †], Kagehiro Magaribuchi[a], Kensuke Seno[a], Mayumi Ito[b], Naoki Hiroyoshi[b]

[a] Laboratory of Mineral Processing and Resources Recycling, Division of Sustainable Resources Engineering, Graduate School of Engineering, Hokkaido University, JAPAN

[b] Laboratory of Mineral Processing and Resources Recycling, Division of Sustainable Resources Engineering, Faculty of Engineering, Hokkaido University, JAPAN

[†]These authors contributed equally to this work

* Corresponding author. Tel.: +81-11-706-6315

E-mail address: ihp2035@gmail.com (Ilhwan Park)

Postal address: Division of Sustainable Resources Engineering, Graduate School of Engineering, Hokkaido University, Kita 13, Nishi 8, Kita-ku, Sapporo 060-8628, Hokkaido, JAPAN

ACCEPTED MANUSCRIPT

Graphical abstract:

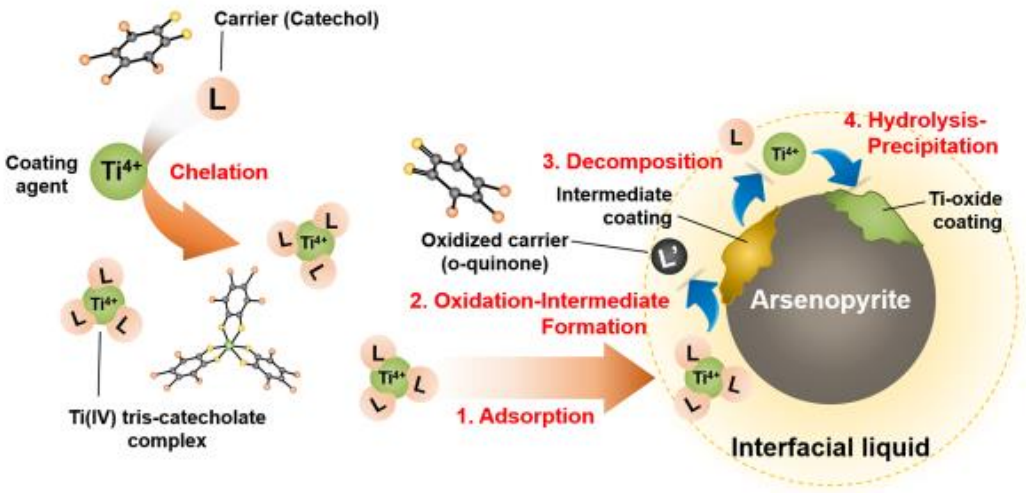

Highlights

- Ti(IV) Tris-catecholate complex was synthesized between pH 5 and 12.
- Ti-based CME limited the release of As from arsenopyrite.
- Mechanism of CME involved adsorption, oxidation, dissociation and coating formation.
- Ti-oxide coating was formed on arsenopyrite.

ABSTRACT

Arsenopyrite is the most common arsenic-bearing sulfide mineral in nature, and its weathering causes the generation of acid mine drainage (AMD) that is accompanied by

ACCEPTED MANUSCRIPT

the release of toxic arsenic (As). To mitigate this problem, carrier-microencapsulation (CME) using titanium (Ti)-catechol complex (*i.e.*, Ti-based CME) was investigated to passivate arsenopyrite by forming a protective coating.

Ti^{4+} ion dissolved in sulfuric acid and catechol were used to synthesize Ti(IV) tris-catecholate complex, $[Ti(Cat)_3]^{2-}$, which was stable in the pH range of 5-12. Electrochemical studies on the redox properties of the complex indicate that its oxidative decomposition was a one-step, irreversible process. Based on these results, a detailed 4-step mechanism is proposed to explain the decomposition of $[Ti(Cat)_3]^{2-}$ and formation of TiO_2 coating in Ti-based CME: (1) adsorption, (2) partial oxidation-intermediate formation, (3) non-electrochemical dissociation, and (4) hydrolysis-precipitation. The leaching of As from arsenopyrite was suppressed after CME treatment using the synthesized Ti-catechol complex. Scanning electron microscopy with energy dispersive X-ray spectroscopy (SEM-EDX) and diffuse reflectance infrared Fourier transform spectroscopy (DRIFTS) indicate that arsenopyrite leaching was primarily suppressed because of the formation of an anatase (β-TiO_2)-containing coating.

Keywords: Acid mine drainage, Arsenic, Arsenopyrite, Microencapsulation, Ti-catechol complex

ACCEPTED MANUSCRIPT

1. Introduction

Mining, mineral processing and tunnel construction for roads and railways often generate large amounts of wastes that contain sulfide minerals such as pyrite (FeS_2) and arsenopyrite (FeAsS), which produce acid mine drainage (AMD) when exposed to the environment [1–14]. AMD is very acidic and could further extract heavy metals (*e.g.*, Fe, Cu, Zn, and Pb) from other minerals found in the wastes, which leads to serious environmental problems if left untreated [15–18].

Many techniques have been investigated to prevent the oxidation of sulfide minerals, the majority of which relied on reducing the exposure of sulfidic wastes to oxygenated water. One example is microencapsulation, a technique wherein pyrite is coated with oxidatively stable materials to prevent its reaction with water and oxygen [19], [20]. In one of the microencapsulation techniques introduced by Evangelou [19], hydrogen peroxide (H_2O_2) was used to oxidize ferrous ion (Fe^{2+}), one of the products of pyrite oxidation, to ferric ion (Fe^{3+}) to form insoluble ferric phosphate on the surface of pyrite, which acted as a protective coating against further oxidation. Pyrite oxidation was effectively suppressed by this technique, but if used haphazardly, it could cause the eutrophication of receiving water bodies because of excess phosphate [2]. Moreover,

ACCEPTED MANUSCRIPT

H_2O_2 could not specifically target pyrite in the real wastes leading to unnecessarily large consumption of expensive reagents.

A great improvement to this technique that addressed these two limitations was proposed by Satur *et al.* [21] called carrier-microencapsulation (CME). CME uses a redox-sensitive organic compound to carry and deliver the coating material, usually an insoluble metal(loid) ion, preferentially to the surface of pyrite where it is adsorbed or precipitated to form the protective coating. The dissolution of pyrite and arsenopyrite is electrochemical in nature [25], a process that requires the movement of electrons between distinct anodic and cathodic sites. Because of this special type of dissolution coupled with the unique electrochemical properties of metal(loid)-carrier complexes, CME could target pyrite and arsenopyrite in complex systems containing other minerals like silicates and aluminosilicates that could dramatically reduce unwanted consumption of chemicals during treatment. This technique has been shown to suppress pyrite oxidation as well as pyrite floatability in coal flotation [21–24].

In the first CME study of Satur *et al.* [21], titanium (Ti)-catechol complex was synthesized by mixing TiO_2 minerals (rutile and anatase) and pyrocatechol (1,2-dihydroxybenzene). These authors showed that catechol extracted Ti-ions directly from TiO_2 but extraction efficiency was very low. Although CME was successfully applied to

ACCEPTED MANUSCRIPT

suppress pyrite oxidation in this previous study, the mechanism(s) involved remained unclear because the authors mixed TiO_2 and catechol together with pyrite. In other words, the suppression of pyrite oxidation by Ti-catechol complex was masked by the effects of TiO_2 and "free" catechol. Mineral oxides attached to pyrite could directly minimize its oxidation by protecting cathodic sites from oxidants like dissolved O_2 (DO) and Fe^{3+} [26], [27]. Likewise, free catechol might indirectly suppress pyrite oxidation by consuming DO and forming stable complexes with Fe^{3+} [28], [29]. In addition, the electrochemical properties of free catechol and Ti-catechol complex was not elucidate in detail, so the mechanism involved in Ti-catechol complex formation and oxidative decomposition remains poorly understood.

In this study, we developed a simple and more efficient method to synthesize Ti-catechol complex for CME treatment. We also investigated the effects of pH and molar ratio on the formation of Ti-catechol complex. Electrochemical studies (*i.e.*, cyclic voltammetry and chronoamperometry) were carried out to understand the electrochemical behavior of synthesized Ti-catechol complex and identify the mechanism(s) involved in its oxidative decomposition as well as in its ability to passivate arsenopyrite. Finally, the synthesized Ti-catechol complex was applied to treat arsenopyrite (FeAsS), the most common arsenic-bearing sulfide mineral in nature, that

ACCEPTED MANUSCRIPT

is closely associated with gold and copper mineralization [30–34]. Arsenopyrite was selected because not only it is common in mine wastes but its weathering also leads to the release of toxic arsenic (As) into the environment. Arsenic is a strictly regulated contaminant because of its serious negative human health effects even at very low concentrations (*i.e.*, μg/L levels) [30], [35–38].

2. Materials and methods

2.1. Ti-catechol complex synthesis and characterization

2.1.1. Synthesis method

In our preparation method to synthesize Ti-catechol complex, Ti^{4+} ions and catechol molecules were mixed directly at very acidic condition (pH < 2). Several studies have already reported that Ti-oxides (*i.e.*, rutile, anatase and ilmenite) dissolve in concentrated sulfuric acid solutions [39–41], so we skipped the dissolution part in this study. Instead, Ti-catechol complex was prepared by mixing reagent grade pyrocatechol and in place of TiO_2 dissolved in concentrated H_2SO_4, we used high purity (99.9%) titanium solution (Ti^{4+} in 1M H_2SO_4) (Wako Chemical Co. Ltd., Japan) to avoid the effects of contaminants like Si and Fe that are ubiquitous in TiO_2 ores.

Our preliminary experiments showed that Ti-catechol complex was only synthesized when the very acidic Ti^{4+} and catechol mixture was rapidly neutralized between pH 5 -

ACCEPTED MANUSCRIPT

12. If neutralization was more gradual (*e.g.*, titration), Ti-catechol complex was not formed because Ti^{4+} ions were rapidly precipitated to TiO_2. In the succeeding sections, all Ti-catechol solutions were prepared by "rapid neutralization".

2.1.2. Ti-complex formation with various stoichiometric molar ratios of Ti^{4+} to catechol

Catechol is a strong chelating agent that coordinates with various metal ions (*e.g.,* Ti^{4+}, Fe^{3+}, Cu^{2+}, and *etc.*) to form several metal-catechol complexes (*i.e.*, mono-, bis- and tris-catecholate) [42], [43]. To evaluate the composition of Ti-catechol complex(es) formed during synthesis, 1 mM of Ti^{4+} solution was mixed with varying stoichiometric molar ratios of Ti^{4+} to catechol (1:0-1:5) at 25°C and 200 rpm. After this, the pH of each solution was rapidly adjusted to 9, transferred to a volumetric flask to adjust the precise concentration by adding small amounts of DI water. The solutions were then filtered and analyzed by an inductively coupled plasma atomic emission spectrometer (ICP-AES, ICPE 9820, Shimadzu Corporation, Japan).

2.1.3. Identification of Ti-catechol complex stability

Solutions containing Ti^{4+} only (1 mM Ti^{4+}) and 1:3 molar ratio of Ti^{4+} to catechol (1 mM Ti^{4+} and 3 mM catechol) were prepared at pH values ranging from 0 to 12 to evaluate the formation and stability of Ti-catechol complex. After rapid neutralization and equilibration, the pH were measured and filtrates were collected by filtration

ACCEPTED MANUSCRIPT

through 0.2 μm syringe-driven filters (Sartorius AG, Germany) to remove precipitates and polymerized organic molecules prior to ICP-AES analyses.

2.1.4. Ultraviolet-visible light spectrophotometric measurements

Ultraviolet-visible light (UV-Vis) spectrophotometric measurements (UV-2500 PC, Shimadzu Corporation, Japan) were conducted to identify Ti-catechol complex(es) formed under various conditions. Catechol only and Ti-catechol solutions adjusted to various pH (1, 3, 6 and 9) were measured in the range of 250-550 nm using a single-crystal quartz cell.

2.2. Electrochemical studies

Cyclic voltammetry (CV) measurements were performed using SI 1280B electrochemical measurement unit (Solartron Instruments, UK) with a conventional three-electrode system (Supplementary information, Fig. S1). Platinum (Pt) electrode, platinum wire and Ag/AgCl electrode filled with 3.3 M NaCl were used as working, counter and reference electrodes, respectively. Three types of solutions were measured by CV: 6 mM catechol at pH 5, 6 mM catechol at pH 9 and Ti-catechol solution (2 mM Ti^{4+} and 6 mM catechol) at pH 9, all of which were prepared in 0.1 M Na_2SO_4 as supporting electrolyte. All experiments were carried out at 25°C under nitrogen atmosphere. The CV measurements started after equilibration at the open circuit

ACCEPTED MANUSCRIPT

potential (OCP), and the sweep direction was towards more positive potentials first (*i.e.*, anodic direction) at a scan rate of 5 mV/s for 5 cycles. In addition, CV measurements of Ti-catechol solution (pH 9) at various scan rates of 1, 5 and 30 mV/s were carried out.

Chronoamperometry was performed to identify the products formed when Ti-catechol complex is anodically decomposed. In this experiment, a similar setup as the CV measurements was used but with magnetic stirring at 200 rpm. The Ti-catechol complex solution was first equilibrated at the OCP, and then anodically polarized at +1.0 V vs. SHE for 3 h. After this, the Pt working electrode was analyzed by scanning electron microscopy with energy dispersive X-ray spectroscopy (SEM-EDX, SSX-550, Shimadzu Corporation, Japan) to determine the oxidation products deposited on it.

2.3. Batch leaching experiments

Three types of solutions were used as leachants in the batch leaching experiments: deionized (DI) water (18 MΩ·cm, Milli-Q® Integral Purification System, Merck Millipore, USA) (control), catechol (15 mM catechol), and synthesized Ti-catechol complex (5 mM Ti^{4+} and 15 mM catechol), all of which were adjusted to pH 9 before mixing them with washed arsenopyrite. The washing technique used to remove any oxidized layer formed on arsenopyrite during sample preparation was based on the method developed by McKibben *et al.* [44]. This method involves ultrasonic desliming

ACCEPTED MANUSCRIPT

in methanol, washing with 1.8 M HNO_3, rinsing with DI water, dewatering with acetone, and drying in a vacuum desiccator. For the leaching experiments, 1 g of arsenopyrite and 10 ml of prepared leachant were put in a 50 ml Erlenmeyer flask and shaken in a constant temperature water bath (25℃) at 120 strokes/min under oxic conditions for up to 25 days. All leaching experiments were done in triplicates to ascertain that differences observed were statistically significant. At pre-designated time intervals, samples were collected, and their pH and oxidation-reduction potential (Eh) were measured. The leachates were collected by filtration through 0.2 μm syringe-driven membrane filters, and immediately analyzed using ICP-AES to measure the concentrations of As and Ti. Meanwhile, the residues were thoroughly washed with DI water and vacuum-dried at 40°C for 24 h. After drying, the residues were analyzed by SEM-EDX to observe the surface of leached arsenopyrite. In addition, diffuse reflectance infrared Fourier transform spectroscopy (DRIFTS, FT/IR-6200HFV with DR PR0410-M attachment, Jasco Analytical Instruments, USA) was used to characterize changes in the surface of samples before and after leaching under the following conditions: 1000 scans at a resolution of 4 cm^{-1} and in the range of 400-4000 cm^{-1}.

3. Results and discussion

ACCEPTED MANUSCRIPT

3.1. Evaluation and characterization of Ti-catechol complex

The effects of pH and solution composition on Ti-catechol complex formation and stability are illustrated in Fig. 1. In the absence of catechol, Ti^{4+} ions remained dissolved in solution under strongly acidic conditions (less than pH 2.0) (Fig. 1a). At pH values higher than 3.5, whitish colored particulates were observed and the concentration of Ti^{4+} ions decreased below the detection limit of ICP-AES (0.001 mg/L), which could be attributed to precipitation of Ti^{4+} as titanium oxide (TiO_2). This deduction is supported by thermodynamic considerations as illustrated by the equilibrium log activity-pH diagram of $Ti(OH)_4$ at 25℃ (Fig. 1b), which showed that the stability of Ti^{4+} as the hydrolyzed $Ti(OH)_4$ ion decreases with pH from 0 to 4. With catechol, however, the solubility of Ti^{4+} ion dramatically increased and the plot exhibited three distinct regions (Fig. 1a). Regions I and II have similar trends with those of the Ti^{4+} only solution, indicating that Ti^{4+} ions in Region I exist because of the very acidic pH while the rapid Ti^{4+} concentration decrease in Region II was due primarily to the precipitation of TiO_2. In Region III, Ti^{4+} concentration started increasing after pH 3.5 coincident with the change in color of solution from transparent to light orange, both of which are strong indicators of Ti-catechol complex formation [42]. Over 80% of Ti^{4+} ion remained in aqueous phase above pH 5.5 (Region III), indicating that most of it was complexed with

ACCEPTED MANUSCRIPT

catechol because Ti^{4+} ion alone cannot exist in solution at this pH without any complexation reaction (Fig. 1a and 1b).

To identify the composition of synthesized Ti-catechol complex, solutions of Ti^{4+} and catechol with various molar ratios at pH 9 were investigated. As shown in Fig. 1c, Ti^{4+} concentration increased at higher molar ratios of catechol to Ti^{4+} until the catechol/Ti^{4+} ratio reached 3. These results fitted well with the theoretical curve of Ti^{4+} ion coordinated with three catechol molecules in the tris-catecholate configuration, suggesting that the synthesized Ti-catechol complex was most likely $[Ti(Cat)_3]^{2-}$. The complexation reaction of Ti^{4+} and catechol could be explained as follows:

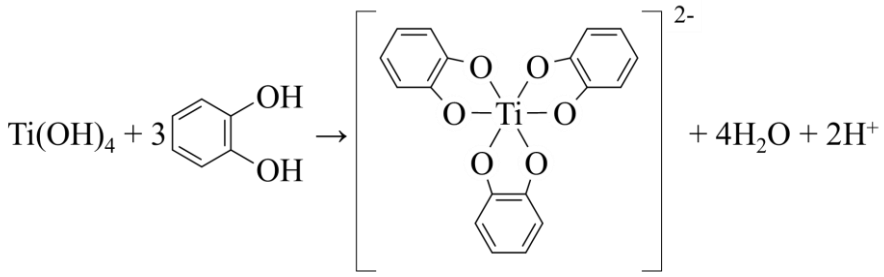

(1)

This deduction is also supported by UV-Vis spectrophotometric measurements of "free" catechol and Ti-catechol solutions at pH 1, 3, 6 and 9 (Fig. 1d). Solutions of Ti^{4+} and catechol at pH 1 and 3 showed only one absorption peak at 274 nm, but at pH 6 and 9, a new peak appeared at around 382 nm. The absorption peak at 274 nm could be attributed to catechol as suggested by the UV-Vis spectra of "free" catechol under various pH conditions (Fig. 1d) while the broad absorption band between 375-389 nm is

ACCEPTED MANUSCRIPT

assigned to the Ti(IV) tris-catecholate complex consistent with the results of other authors [42], [43]. It is also noteworthy that the $[Ti(Cat)_3]^{2-}$ absorption band was only apparent at pH 6 and 9, which is in strong agreement with the results shown in Fig. 1a.

3.2. Mechanism of Ti-catechol decomposition and coating formation

Cyclic voltammetry (CV), a type of potentiodynamic electrochemical technique that provides insights into the redox reactions of compounds in solutions, was carried out to understand how "free" catechol and Ti-catechol complex decompose under conditions that roughly simulate those existing on the surface of arsenopyrite during oxidation. Cyclic voltammogram of catechol at pH 5 (Fig. 2a-1) showed an anodic peak at 770 mV vs. SHE (A_1) and a cathodic peak at 500 mV (C_1), which are consistent with the well documented reversible redox reaction of this organic compound [29], [47], [48]. Catechol is oxidized to quinone (1,2-Benzoquinone) during the anodic sweep at 770 mV and is reduced back to catechol in the succeeding cathodic sweep at 500 mV (Eq. (2)). In contrast, the voltammogram of catechol at pH 9 (Fig. 2a-2) showed two anodic peaks at 780 (A1') and 260 mV (A_2') but only one cathodic peak at 500 mV (C_1'). The peaks at A_1' and C_1' were similar to that of catechol at pH 5 while the additional anodic peak at ca. 260 mV (A_2') could be attributed to oxidation of semi-quinone (Eq. (3)) formed during solution preparation. The strong presence of semi-quinone at pH 9 could be

ACCEPTED MANUSCRIPT

explained by the following reasons: (1) faster oxidation rate of catechol to semi-quinone under alkaline conditions by O_2 [49], and (2) greater stability of semi-quinone because of its lower one-electron reduction potential at higher pH [48].

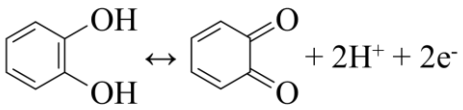

(2)

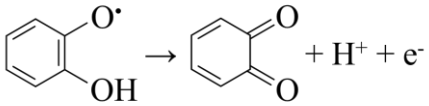

(3)

A new anodic peak at ca. 680 mV (A_1'') appeared in the cyclic voltammogram of Ti-catechol complex (Fig. 2a-3) indicating that the synthesized Ti-catechol complex, $[Ti(Cat)_3]^{2-}$, could undergo anodic decomposition. The cathodic peak observed at 440 mV (C_1'') was most likely due to the reduction of quinone to catechol as discussed earlier. In the second cycle (Fig. 2a-3), however, the anodic peak decreased and shifted towards higher potentials compared with that of the first cycle. Succeeding cycles (*i.e.*, 3rd and 4th) also showed continuous shift and decrease of the anodic peak until it virtually disappeared on the fifth cycle. This gradual decrease of the anodic peak could be attributed to the decreasing amount of Ti-catechol complex due to its oxidative decomposition near the surface of working electrode, which was not regenerated from oxidation products in the succeeding cathodic sweep. This means that the oxidative

ACCEPTED MANUSCRIPT

decomposition of Ti-catechol complex is irreversible. Furthermore, shifting of the anodic peak may suggest that surface of the platinum electrode is gradually being covered by oxidation products.

Some metal tris-catecholate complexes like those of Mn(IV) and Fe(III) have been reported to decompose sequentially [50], so to determine whether this is also the case for the synthesized Ti-catechol complex, CV measurements at several scan rates were conducted to change the extent of oxidation-reduction reactions. Despite the various scan rates (1 to 30 mV/s), however, only one anodic peak was observed (Fig. 2b), indicating that the oxidative decomposition of Ti-catechol complex occurred via a one-step process and not sequentially. Satur *et al.* [21] proposed that the one-step oxidation of Ti-catechol complex occur via simultaneous oxidation of the three catechol molecules coordinated with Ti^{4+}, which would be precipitated as Ti-hydroxide/oxide because of its very low solubility at pH>4. If their hypothesis is correct, then the product after oxidation would be composed almost entirely of Ti-hydroxide/oxide. To verify this, chronoamperometry was carried out at 1.0 V vs. SHE for 3 h to generate enough oxidation products on the Pt electrode for SEM-EDX analysis. As illustrated in Fig. 3, there were two distinct materials observed in the coating formed on Pt electrode after chronoamperometry: (1) a high carbon-containing substance (Ti-O-C), and (2) a

ACCEPTED MANUSCRIPT

high titanium and oxygen-containing material (Ti-O). These materials are definitely oxidation products of Ti-catechol complex decomposition because they were not observed when the same experiment was done without applying any potential (Supplementary information, Fig. S2). Based on these results, decomposition of Ti-catechol is much more complicated than the earlier mechanism proposed by Satur *et al.* [21].

In the structure of Ti(IV) tris-catecholate complex (Fig. 4), one catechol molecule is "normally" coordinated with the central Ti^{4+} ion while the remaining two molecules are coordinated with distortions because of unpaired electrons in two oxygen atoms (O_4 and O_5) [42]. These oxygen atoms, O_4 and O_5, are relatively more reactive than the others, so during anodic decomposition, Ti-O_4 and/or Ti-O_5 bonds are most probably attacked first and dislodged, resulting in the formation of Ti(IV) mono- and/or bis-catecholate complex (Eqs. (4) – (5)). Mono- and bis-catecholate complexes have been reported for Mn(IV) and Fe(III) but not for Ti(IV), which could indicate that $[Ti(Cat)]^{2+}$ and/or $[Ti(Cat)_2]$ complex(es) are very unstable [43], [50]. Another possible explanation is the formation of more stable polymerized metal-organic molecule by partially oxidized Ti-catechol complexes. In a recent paper of Bazhenova *et al.* [51], a new family of polymerized Ti-catechol complexes were introduced that contain both Ti^{4+} mono- and

ACCEPTED MANUSCRIPT

bis-catecholate complexes as their "elementary" components, suggesting that the presence of Ti-O-C "intermediate" was likely the result of partial oxidation-polymerization reactions.

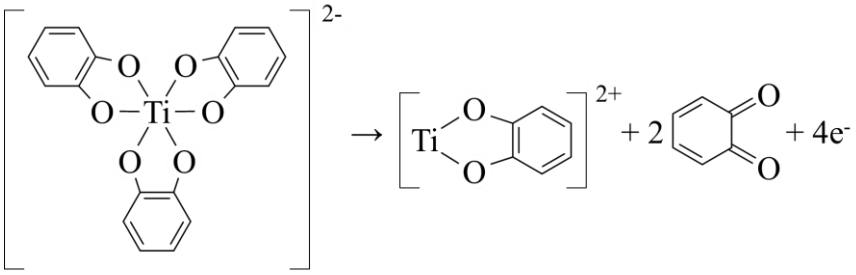

(4)

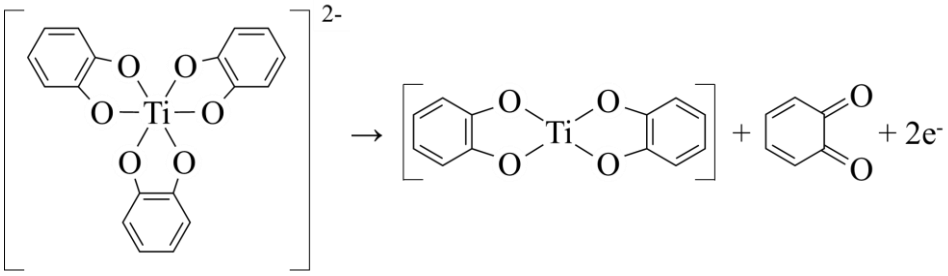

(5)

Ti-O in the coating, observed as regions with darker hues in the BSE image with very strong Ti and O signals (Fig. 3), was most likely formed by the decomposition of Ti-O-C "intermediate", which did not require electron transfer. This is consistent with the cyclic voltammogram of Ti-catechol complex showing a one-step electrochemical reaction (*i.e.*, $[Ti(Cat)_3]^{2-}$ oxidation → Ti-O-C "intermediate" formation) (Fig. 2). Finally, Ti^{4+} ion released from intermediate was precipitated as Ti-hydroxide/oxide that formed the Ti-O material in the Ti-O-C coating.

Based on these results, a three-step mechanism is proposed for the decomposition of Ti-catechol complex (Fig. 5). In Step 1, Ti-catechol complex is partially oxidized, most

ACCEPTED MANUSCRIPT

probably via the Ti-O distorted bonds, and forms an intermediate phase. After this, the intermediate is gradually dissociated until "free" Ti^{4+} ion is released (Step 2). In the final step (Step 3), "free" Ti^{4+} ion is hydrolyzed and precipitated to form Ti-oxyhydroxide coatings.

3.3. Ti-based CME treatment of arsenopyrite

The arsenopyrite sample used in this study was obtained from Toroku Mine, Miyazaki, Japan. XRD pattern of the sample shows that it is mainly composed of arsenopyrite with pyrite and quartz as minor minerals (Supplementary information, Fig. S3). Its chemical composition is 32.6, 30.9 and 20.1% of Fe, As and S, respectively, and these values translate to ca. 67% of arsenopyrite, 13% of pyrite and 15% of quartz (Supplementary information, Table S1).

Fig. 6 shows the evolution of pH, Eh, and concentrations of As and Ti in DI water (control), catechol only and Ti-catechol complex solution (CME). In the control, the pH rapidly decreased from 9 to 3.5 after 1 day due to the production of hydrogen ion by arsenopyrite oxidation [29], [37], which is consistent with the redox potential (Eh) increase from ca. 250 to 500 mV (Fig. 6a and 6b). The oxidation of arsenopyrite was also apparent in the rapid concentration increase of As in the control with time that reached ca. 1000 mg/L after 7 days (Eqs. (6) – (8)). After this period, the change in As

ACCEPTED MANUSCRIPT

concentration with time became statistically insignificant indicating that apparent equilibrium was reached.

$$4FeAsS_{(s)} + 11O_{2(aq)} + 6H_2O \rightarrow 4Fe^{2+}_{(aq)} + 4H_3AsO_{3(aq)} + 4SO_4^{2-}{}_{(aq)} \quad (6)$$

$$4Fe^{2+}_{(aq)} + O_{2(aq)} + 4H^{+}_{(aq)} \rightarrow 4Fe^{3+}_{(aq)} + 2H_2O \quad (7)$$

$$FeAsS_{(s)} + 13Fe^{3+}_{(aq)} + 8H_2O \rightarrow 14Fe^{2+}_{(aq)} + H_3AsO_{4(aq)} + SO_4^{2-}{}_{(aq)} + 13H^{+}_{(aq)} \quad (8)$$

In the presence of catechol, As concentration was lower and the pH was higher than those of the control (Fig. 6a and 6c), which means that arsenopyrite oxidation was somehow limited by this organic compound. This suppressive effect could be explained by two possible mechanisms. First, catechol adsorption to the surface of arsenopyrite could suppress the overall dynamics of arsenopyrite oxidation by protecting the mineral from oxidants. This "direct" effect of catechol is most likely similar to that previously reported by Lalvani *et al.* [52] and Belzile *et al.* [53] on pyrite passivation by humic acids, large organic molecules that contain catechol as one of their most common functional groups. Noteworthy in the results was the continuous increase in As concentration with time in the catechol only solution, which suggests that although arsenopyrite oxidation was minimized, the mineral was not passivated by catechol (Fig. 6c). Second, catechol could "indirectly" suppress arsenopyrite oxidation by consuming DO and complexing with Fe^{3+}, both of which are essential oxidants of arsenopyrite.

ACCEPTED MANUSCRIPT

According to Pracht *et al.* [28], catechol consumes DO and metal ions such as Fe^{3+} in its oxidation to quinone (Eqs. (9) – (10)). Catechol has also been reported that form several stable complexes with Fe^{3+} (*e.g.*, Eq. (11)) preventing it from directly acting as an oxidant of arsenopyrite [29]. The combined effects of adsorption, consumption of oxidants and formation of Fe(III)-catechol complexes could explain the decrease in As concentration observed in the presence of catechol.

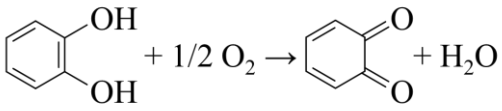

(9)

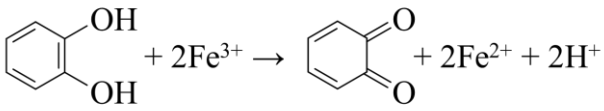

(10)

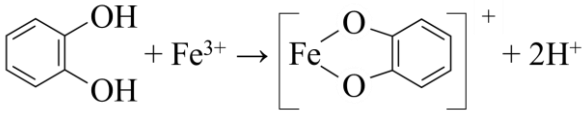

(11)

The amounts of As released from arsenopyrite was even lower in Ti-catechol complex solution (CME) compared with the other two cases (Fig. 6c). After 25 days, As concentration in CME was ca. 330 mg/L, which was roughly four-fold lower than the control (1150 mg/L) and less than half of that in catechol only solution (880 mg/L). The pH was also higher in CME compared with the other cases while Eh was the lowest (Fig. 6a and 6b). These results suggest that the substantial decrease in As release from

ACCEPTED MANUSCRIPT

arsenopyrite could be attributed to passivation of the mineral itself by Ti-catechol complex. The passivation of arsenopyrite was closely related to Ti^{4+} precipitation that was apparent in the concentration decrease of dissolved Ti with time, which was not observed in Ti-catechol solution without arsenopyrite (Fig. 6d). SEM-EDX results also showed that arsenopyrite in CME after 25 days exhibited strong signals of Ti and O (Fig. 7). Coating coverage was estimated using image analysis of Ti elemental maps of SEM-EDX and based on the results, Ti-based CME roughly covered 60% of arsenopyrite (Supplementary information, Fig. S4 and Table S2). The nature of this passivation layer was characterized using DRIFTS, a surface-sensitive technique able to identify molecular coordinations of ions and molecules in the structure of minerals [54] including the very thin oxidation products of pyrite oxidation [19], [26], [55]. The DRIFTS spectra of washed arsenopyrite and leached residues (control, catechol and CME) show that several oxidation products were formed on arsenopyrite (Fig. 8a). Absorption bands at 457 and 792 cm^{-1} are assigned to vibrations of Fe-As and arsenate (O-As-O), respectively. The stronger signal of arsenate (792 cm^{-1}) in the control indicates that arsenopyrite oxidation was more extensive in DI water compared with those in the other cases [56], [57]. Absorption bands at 569, 487 and 478 cm^{-1} are assigned to Fe-O bonds of iron oxide and the peak at 1371 cm^{-1} is most likely due to

ACCEPTED MANUSCRIPT

Fe^{3+}-OH band of Fe^{3+}-hydroxides or oxyhydroxides [26], [57], [58]. Vibrations of sulfate coordinated with Fe^{3+} and Fe^{2+} were also observed at 1050 and 1163 cm^{-1}, respectively [54–58]. The wide peak between 1115-1230 cm^{-1} is assigned to the vibrations of C-H (1165 cm^{-1}), O-H (1187 cm^{-1}), and C-O (1193 cm^{-1}), indicating two possibilities: (1) adsorbed catechol on arsenopyrite [59], and (2) an "intermediate" phase formed on arsenopyrite by the partial decomposition of Ti-catechol complex as discussed previously. The deconvoluted spectrum between 500 and 400 cm^{-1} of arsenopyrite leached in Ti-catechol complex solution (Fig. 8b) shows several absorption bands at 488, 474, 445 and 427 cm^{-1}, which are consistent with Ti-O vibrations of anatase (β-TiO_2) [60–63]. This means that the Ti and O signals detected by SEM-EDX were likely due to the Ti-oxide coating formed on arsenopyrite that passivated the mineral itself and limited the release of As.

4. Conclusion

This study investigated the formation of Ti-catechol complex, its electrochemical properties and its application to the CME treatment of arsenopyrite. The findings of this study are summarized as follows:

1) Ti-catechol complex was successfully synthesized by rapid neutralization of very acidic Ti^{4+} and catechol solutions to pH > 5.

ACCEPTED MANUSCRIPT

2) The synthesized Ti-catechol complex had a tris-catecholate configuration, $[Ti(Cat)_3]^{2-}$, and was relatively stable between pH 5 and 12.

3) $[Ti(Cat)_3]^{2-}$ could be oxidized at 680 mV most probably via the partial oxidation of either one or both of catechol molecules with distorted Ti-O bonds. The partially oxidized complex(es) likely reacted with each other to form an "intermediate" phase composed of Ti, O and C.

4) Under certain conditions, the "intermediate" could be completely dissociated, which released "free" Ti^{4+} ion into solution that rapidly precipitated as TiO_2.

5) Ti-based CME suppressed the release of As from arsenopyrite by coating the mineral with Ti-oxide.

6) The new method to synthesize Ti-catechol complex and the added insights into the mechanisms of CME treatment could help in the design of practical approaches to mitigate not only the release of As but also to suppress AMD generation.

Acknowledgments

A part of this study was financially supported by the Japan Society for the Promotion of Science (JSPS) grant-in-aid for scientific research (Grant numbers: 26820390, 17H03503 and 17K12831).

References

ACCEPTED MANUSCRIPT

[1] D. Banks, P.L. Younger, R.T. Arnesen, E.R. Iversen and S.B. Banks, Mine-water chemistry: the good, the bad and the ugly, Environ. Geol. 32 (1997) 157-174.

[2] A.R. Elsetinow, M.J. Borda, M.A.A. Schoonen and D.R. Strongin, Suppression of pyrite oxidation in acidic aqueous environments using lipids having two hydrophobic tails, Adv. Environ. Res. 7 (2003) 969-974.

[3] D.B. Johnson and K.B. Hallberg, Acid mine drainage remediation options: a review, Sci. Total Environ. 338 (2005) 3-14.

[4] C.B. Tabelin and T. Igarashi, Mechanisms of arsenic and lead release from hydrothermally altered rock, J. Hazard. Mater. 169 (2009) 980-990.

[5] C.B. Tabelin, T. Igarashi and R. Takahashi, The roles of pyrite and calcite in the mobilization of arsenic and lead from hydrothermally altered rocks excavated in Hokkaido, Japan, J. Geochem. Explor. 119 (2012a) 17-31.

[6] C.B. Tabelin, A.H.M. Basri, T. Igarashi and T. Yoneda, Removal of arsenic, boron, and selenium from excavated rocks by consecutive washing, Water Air Soil Poll. 223 (2012b) 4153-4167.

[7] C.B. Tabelin, T. Igarashi, T. Arima, D. Sato, T. Tatsuhara and S. Tamoto, Characterization and evaluation of arsenic and boron adsorption onto natural geologic materials, and their application in the disposal of excavated altered rock, Geoderma 213 (2012c) 163-172.

[8] C.B. Tabelin, T. Igarashi and R. Takahashi, Mobilization and speciation of arsenic from hydrothermally altered rock in laboratory column experiments under ambient conditions, Appl. Geochem 27 (2012d) 326-342.

[9] C.B. Tabelin, A. Hashimoto, T. Igarashi and T. Yoneda, Leaching of boron, arsenic and selenium from sedimentary rocks: I. Effects of contact time, mixing speed and liquid-to-solid ratio, Sci. Total Environ. 472 (2014a) 620-629.

[10] C.B. Tabelin, A. Hashimoto, T. Igarashi and T. Yoneda, Leaching of boron, arsenic and selenium from sedimentary rocks: II. pH dependence, speciation and mechanisms of release, Sci. Total Environ. 473-474 (2014b) 244-253.

[11] C.B. Tabelin, R. Sasaki, T. Igarashi, I. Park, S. Tamoto, T. Arima, M. Ito and N. Hiroyoshi, Simultaneous leaching of arsenite, arsenate, selenite and selenite, and their migration in tunnel-excavated sedimentary rocks: I. Column experiments under intermittent and unsaturated flow, Chemosphere 186 (2017a) 558-569.

ACCEPTED MANUSCRIPT

[12] C.B. Tabelin, R. Sasaki, T. Igarashi, I. Park, S. Tamoto, T. Arima, M. Ito and N. Hiroyoshi, Simultaneous leaching of arsenite, arsenate, selenite and selenite, and their migration in tunnel-excavated sedimentary rocks: II. Kinetic and reactive transport modeling, Chemosphere (2017b) https://doi.org/10.1016/j.chemosphere.2017.08.088 (Accepted).

[13] T. Tatsuhara, T. Arima, T. Iagarashi and C.B. Tabelin, Combined neutralization-adsorption system for the disposal of hydrothermally altered excavated rock producing acidic leachate with hazardous elements, Eng. Geol. 139-140 (2012) 76-84.

[14] S. Tamoto, C.B. Tabelin, T. Igarashi, M. Ito and N. Hiroyoshi, Short and long term release mechanisms of arsenic, selenium and boron from tunnel-excavated sedimentary rock under in situ conditions, J. Contam. Hydrol. 175-176 (2015) 60-71.

[15] A. Akcil and S. Koldas, Acid Mine Drainage (AMD): causes, treatment and case studies, J. Clean. Prod. 14 (2006) 1139-1145.

[16] B. Gazea, K. Adam and A. Kontopoulos, A Review of Passive Systems for the Treatment of Acid Mine Drainage, Miner. Eng. 9 (1996) 23-42.

[17] N.F. Gray, Environmental impact and remediation of acid mine drainage: a management problem, Environ. Geol. 30 (1997) 62-71.

[18] A.N. Shabalala, S.O. Ekolu, S. Diop and F. Solomon, Pervious concrete reactive barrier for removal of heavy metals fromacid mine drainage − column study, J. Hazard. Mater. 323 (2017) 641-653.

[19] V.P. Evangelou, Pyrite oxidation and its control, CRC press, Boca Raton, FL (1995).

[20] V.P. Evangelou, Pyrite microencapsulation technologies: Principles and potential field application, Ecol. Eng. 17 (2001) 165-178.

[21] J. Satur, N. Hiroyoshi, M. Tsunekawa, M. Ito and H. Okamoto, Carrier-microencapsulation for preventing pyrite oxidation, Int. J. Miner. Eng. 83 (2007) 116-124.

[22] R.K.T. Jha, J. Satur, N. Hiroyoshi, M. Ito and M. Tsunekawa, Carrier-microencapsulation using Si-catechol complex for suppressing pyrite floatability, Miner. Eng. 21 (2008) 889-893.

[23] R.K.T. Jha, J. Satur, N. Hiroyoshi, M. Ito and M. Tsunekawa, Suppression of floatability of pyrite in coal processing by carrier microencapsulation, Fuel Process. Technol. 92 (2011) 1032-1036.

[24] M.D. Yuniati, K. Kitagawa, T. Hirajima, H. Miki, N. Okibe and K. Sasaki, Suppression of pyrite oxidation in acid mine drainage by carrier microencapsulation using liquid product of

ACCEPTED MANUSCRIPT

hydrothermal treatment of low-rank coal, and electrochemical behavior of resultant encapsulating coatings, Hydrometallurgy 158 (2015) 83-93.

[25] J.D. Rimstidt , D.J. Vaughan, Pyrite oxidation: a state-of-the-art assessment of the reaction mechanism, Geochim. Cosmochim. Acta 67 (2003) 873-880.

[26] C.B. Tabelin, S. Veerawattananun, M. Ito, N. Hiroyoshi and T. Igarashi, Pyrite oxidation in the presence of hematite and alumina: I. Batch leaching experiments and kinetic modeling calculations, Sci. Total Environ. 580 (2017a) 687-698.

[27] C.B. Tabelin, S. Veerawattananun, M. Ito, N. Hiroyoshi and T. Igarashi, Pyrite oxidation in the presence of hematite and alumina: II. Effects on the cathodic and anodic half-cell reactions, Sci. Total Environ. 581-582 (2017b) 126-135.

[28] J. Pracht, J. Boenigk, M. Isenbeck-Schröter, F. Keppler and H.F. Schöler, Abiotic Fe(III) induced mineralization of phenolic substances, Chemosphere 44 (2001) 613-619.

[29] N. Schweigert, A.J.B. Zehnder and R.I.L. Eggen, Chemical properties of catechols and their molecular modes of toxic action in cells, from microorganisms to mammals, Environ. Microbiol. 3 (2001) 81-91.

[30] C.L. Corkhill and D.J. Vaughan, Arsenopyrite oxidation - A review, Appl. Geochem. 24 (2009) 2342-2361.

[31] S. Coussy, M. Benzaazoua, D. Blanc, P. Moszkowicz and B. Bussière, Arsenic stability in arsenopyrite-rich cemented paste backfills: A leaching test-based assessment, J. Hazard. Mater. 185 (2011) 1467-1476.

[32] A.B.M.R. Islam, J.P. Maity, J. Bundschuh, C.Y. Chen, B.K. Bhowmik and K. Tazaki, Arsenic mineral dissolution and possible mobilization in mineral-microbe-groundwater environment, J. Hazard. Mater. 262 (2013) 989-996.

[33] A. Murciego, E. Álvarez-Ayuso, E. Pellitero, MªA. Rodríguez, A. García-Sánchez, A. Tamayo, J. Rubio, F. Rubio and J. Rubin, Study of arsenopyrite weathering products in mine wastes from abandoned tungsten and tin exploitations, J. Hazard. Mater. 186 (2011) 590-601.

[34] K.A. Salzsauler, N.V. Sidenko and B.L. Sherriff, Arsenic mobility in alteration products of sulfide-rich, arsenopyrite-bearing mine wastes, Snow Lake, Manitoba, Canada, Appl. Geochem. 20 (2005) 2303-2314.

[35] A. Basu and M.E. Schreiber, Arsenic release from arsenopyrite weathering: Insights from sequential extraction and microscopic studies, J. Hazard. Mater. 262 (2013) 896-904.

ACCEPTED MANUSCRIPT

[36] C.K. Jain and I. Ali, Arsenic: Occurrence, toxicity and speciation techniques, Water Res. 34 (2000) 4304-4312.

[37] D. Mohan and C.U. Pittman Jr., Arsenic removal from water/wastewater using adsorbents - A critical review, J. Hazard. Mater. 142 (2007) 1-53.

[38] H.W. Nesbitt, I.J. Muir and A.R. Pratt, Oxidation of arsenopyrite by air and air-saturated, distilled water, and implications for mechanism of oxidation, Geochim. Cosmochim. Acta 59 (1995) 1773-1786.

[39] S. Agatzini-Leonardou, P. Oustadakis, P.E. Tsakiridis and Ch. Markopoulos, Titanium leaching from red mud by diluted sulfuric acid at atmospheric pressure, J. Hazard. Mater. 157 (2008) 579-586.

[40] S. He, H. Sun, D. Tan and T. Peng, Recovery of titanium compounds from Ti-enriched product of alkali melting Ti-bearing blast furnace slag by dilute sulfuric acid leaching, Procedia Environ. Sci. 31 (2016) 977-984.

[41] F.C. Meng, T.Y. Xue, Y.H. Liu, G.Z. Zhang and T. Qi, Recovery of titanium from undissolved residue (tionite) in titanium oxide industry via NaOH hydrothermal conversion and H_2SO_4 leaching, Trans. Nonferrous Met. Soc. China 26 (2016) 1696-1705.

[42] B.A. Borgias, S.R. Cooper, Y.B. Koh and K.N. Raymond, Synthetic, Structural, and Physical Studies of Titanium Complexes of Catechol and 3,5-Di-*tert*-butylcatechol, Inorg. Chem. 23 (1984) 1009-1016.

[43] M.J. Sever and J.J. Wilker, Visible absorption spectra of metal-catecholate and metal-tironate complexes, Dalton Trans. (2004) 1061-1072.

[44] M.A. McKibben, B.A. Tallant and J.K. del Angel, Kinetics of inorganic arsenopyrite oxidation in acidic aqueous solutions, Appl. Geochem. 23 (2008) 121-135.

[45] C.M. Bethke, The Geochemist's Workbench – A User's Guide to Rxn, Act2, Tact, React and Gtplot, University of Illinois, Urbana, Illinois, 1992.

[46] J.P. Gustafsson, Visual MINTEQ thermodynamic databases in GWB format, http://vminteq.lwr.kth.se, 2010 (accessed 08.04.2010).

[47] J.C. Danilewicz, Review of Oxidative Processes in Wine and Value of Reduction Potentials in Enology, Am. J. Enol. Vitic. 63 (2012) 1-10.

[48] J. Yang, M.A.C. Stuart and M. Kamperman, Jack of all trades: versatile catechol crosslinking mechanisms, Chem. Soc. Rev. 43 (2014) 8271-8298.

ACCEPTED MANUSCRIPT

[49] C.I. Wright and H.S. Mason, The oxidation of catechol by tyrosinase, J. biol. Chem. 165 (1946) 45-53.

[50] K.A. Boles, Electrochemistry of tris(tetrachlorocatecholate) complexes of manganese, iron, and cobalt, Chemistry & biochemistry graduate theses & dissertations (2014).

[51] T.A. Bazhenova, N.V. Kovaleva, G.V. Shilov, G.N. Petrova and D.A. Kuznetsov, A Family of Titanium Complexes with Catechol Ligands: Structural Investigation and Catalytic Application, Eur. J. Inorg. Chem. 33 (2016) 5215-5221.

[52] S.B. Lalvani, B.A. Deneve and A. Weston, Passivation of pyrite due to surface treatment, Fuel 69 (1990) 1567-1569.

[53] N. Belzile, S. Maki, Y.W. Chen and D. Goldsack, Inhibition of pyrite oxidation by surface treatment, Sci. Total Environ. 196 (1997) 177-186.

[54] L. Carlson, J.M. Bingham, U. Schwertmann, A. Kyek and F. Wagner, Scavenging of As from Acid Mine Drainage by Schwertmannite and Ferrihydrite: A Comparison with Synthetic Analogues, Environ. Sci. Technol. 36 (2002) 1712-1719.

[55] M.J. Borda, D.R. Strongin, and M.A. Schoonen, A vibrational spectroscopic study of the oxidation of pyrite by molecular oxygen, Geochim. Cosmochim. Acta 68 (2004) 1807-1813.

[56] M. Achimovičová and P. Baláž, Influence of mechanical activation on selectivity of acid leaching of arsenopyrite, Hydrometallurgy 77 (2005) 3-7.

[57] M.B.M. Monte, A.J.B. Dutra, C.R.F. Albuquerque Jr., L.A. Tondo and F.F. Lins, The influence of the oxidation state of pyrite and arsenopyrite on the flotation of an auriferous sulphide ore, Miner. Eng. 15 (2002) 1113-1120.

[58] I.V. Chernyshova, An in situ FTIR study of galena and pyrite oxidation in aqueous solution, J. Electroanal. Chem. 558 (2003) 83-98.

[59] F.J. Ramírez and J.T. López Navarrete, Normal coordinate and rotational barrier calculations on 1,2-dihydroxybenzene, Vib. Spectrosc. 4 (1993) 321-334.

[60] M.J. Alam and D.C. Cameron, Preparation and Characterization of TiO_2 Thin Films by Sol-Gel Method, J. Sol-Gel Sci. Technol. 25 (2002) 137-145.

[61] S. Bagheri, K. Shameli and S.B.A. Hamid, Synthesis and Characterization of Anatase Titanium Dioxide Nanoparticles Using Egg White Solution via Sol-Gel Method, J. Chem. (2013) 1-5.

[62] Y. Djaoued, S. Badilescu, P.V. Ashrit, D. Bersani, P.P. Lottici and R. Brüning, Low

ACCEPTED MANUSCRIPT

Temperature Sol-Gel Preparation of Nanocrystalline TiO2 Thin Films, J. Sol-Gel Sci. Technol. 24 (2002 a) 247-254.

[63] Y. Djaoued, S. Badilescu, P.V. Ashrit, D. Bersani, P.P. Lottici and J. Robichaud, Study of Anatase to Rutile Phase Transition in Nanocrystalline Titania Films, J. Sol-Gel Sci. Technol. 24 (2002 b) 255-264.

ACCEPTED MANUSCRIPT

Figure Captions

Fig. 1. Properties of synthesized Ti-catechol complex: (a) Ti^{4+} ion stability with pH in the presence and absence of catechol, (b) Log *a* – pH predominance diagram of $Ti(OH)_4$ at 25°C and 1.013 bars created using the Geochemist's Workbench® with MINTEQ database [45] and [46], (c) Ti^{4+} ion stability as a function of molar ratio of Ti^{4+} to catechol, (d) UV-Vis spectra of "free" catechol and Ti-catechol solutions at pH 1, 3, 6 and 9.

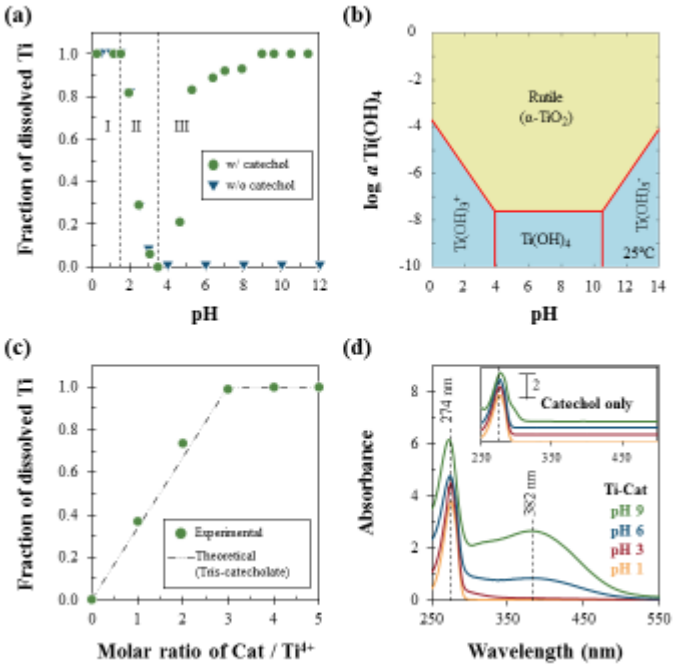

Fig. 2. Cyclic voltammograms of (a) catechol only and Ti-catechol solution at a scan rate of 5 mV/s, (a-1) catechol at pH 5, (a-2) catechol at pH 9, (a-3) Ti-catechol at pH 9, and (b) Ti-catechol solution at pH 9 with various scan rates (1 mV/s (b-1), 5 mV/s (b-2), and 30 mV/s (b-3)).

ACCEPTED MANUSCRIPT

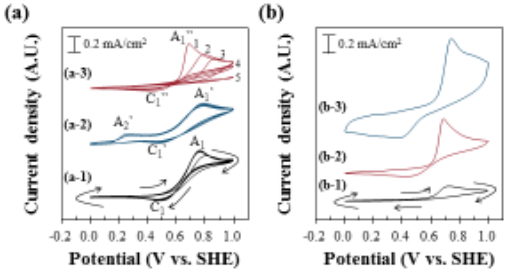

Fig. 3. SEM-EDX analysis of Pt electrode after chronoamperometry at 1.0 V vs. SHE for 3 h: (a-1) SEM photomicrograph and (a-2) energy dispersive X-ray spectra of several points, (b-1) SEM photomicrograph and elemental maps of Pt (b-2), C (b-3), Ti (b-4), and O (b-5).

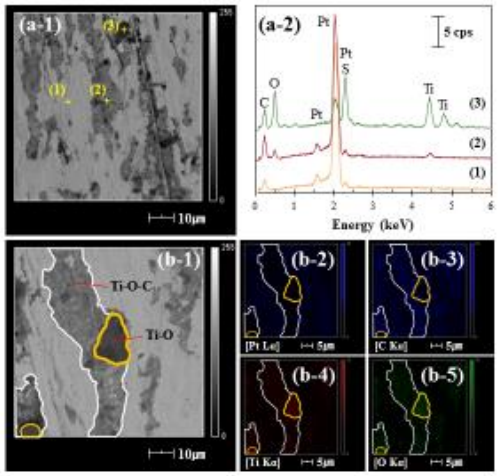

ACCEPTED MANUSCRIPT

Fig. 4. Molecular structure of Ti(IV) tris-catecholate complex [42].

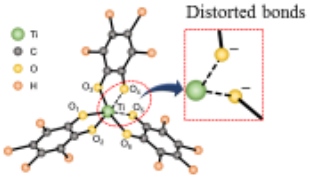

Fig. 5. A schematic diagram of the anodic decomposition of Ti-catechol complex.

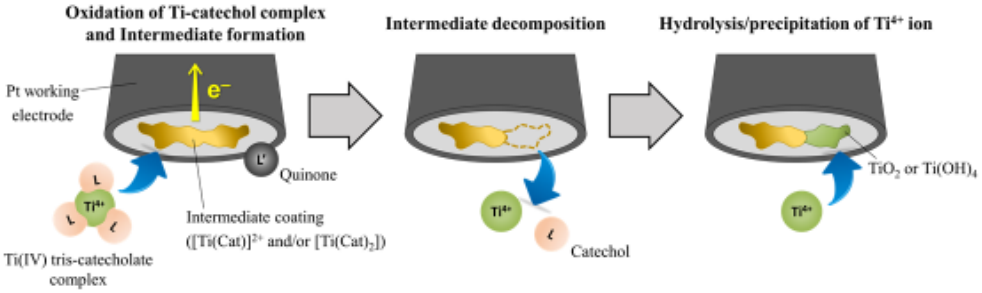

ACCEPTED MANUSCRIPT

Fig. 6. Leaching of arsenopyrite in DI water (control), catechol only and Ti-catechol complex (CME): evolution of (a) pH and (b) Eh, and changes in the concentrations of (c) As and (d) Ti with time.

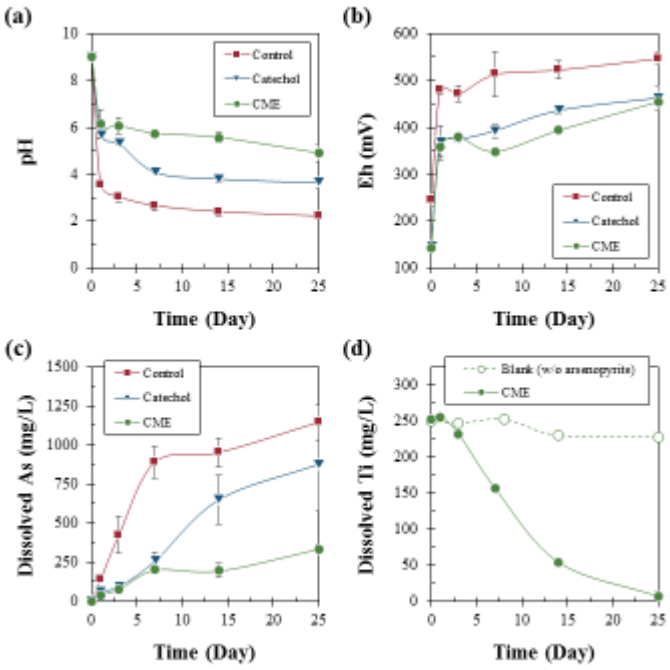

Fig. 7. SEM-EDX analysis of arsenopyrite after Ti-based CME treatment: (a) SEM photomicrograph, elemental maps of (b) Fe, (c) As, (d) S, (e) Ti and (f) O, and (g) energy dispersive X-ray spectrum of scanned area.

ACCEPTED MANUSCRIPT

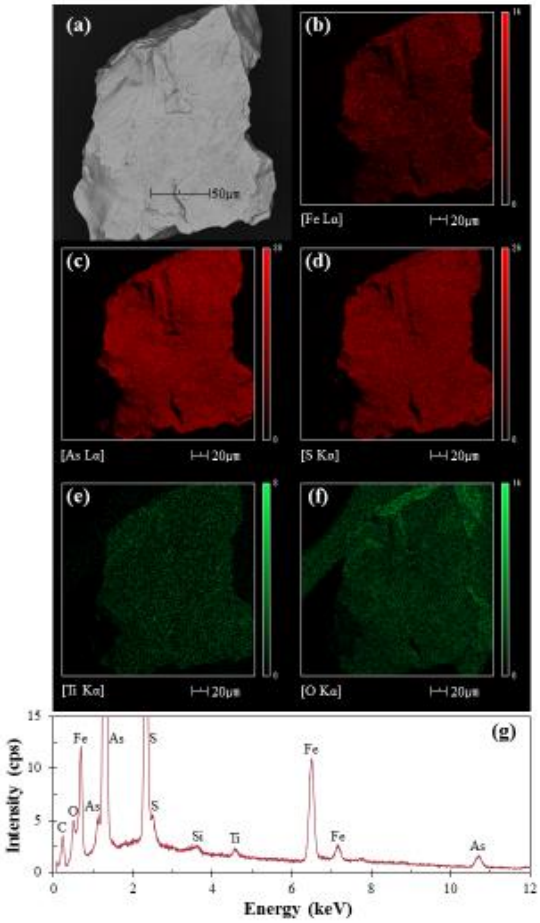

ACCEPTED MANUSCRIPT

Fig. 8. DRIFTS spectra of arsenopyrite before and after 25 days of leaching experiments: (a) spectra of washed arsenopyrite and residues leached in DI water (control), catechol only and Ti-catechol solution (CME), and (b) deconvoluted spectrum of CME-treated arsenopyrite. Note that the scale of (a) and (b) are 0.05 and 0.005, respectively.